1 **Xylem traits and growth phenology predict growth and mortality response to defoliation in**

2 **temperate forests**

3

4 **JANE R. FOSTER**[a1*]

5 J.R. Foster (Corresponding author)

6 [a] University of Wisconsin Madison

7 Department of Forest and Wildlife Ecology

8 120 Russell Labs

9 1630 Linden Dr

10 Madison WI 53706-1520

11 USA

12 [1](Present address)

13 University of Minnesota

14 Department of Forest Resources

15 115 Green Hall

16 1530 Cleveland Ave. N.

17 St. Paul, MN 55108

18 email: jrfoster@umn.edu

19 **Running headline:** GROWTH AND MORTALITY RESPONSE TO DEFOLIATION

20 **Key-words:** ecophysiology, forest dynamics, forest models, hydraulic architecture, insect

21 disturbance, non-structural carbohydrates, phenology, plant population and community

22 dynamics, plant-herbivore interactions

23 **Abstract**

24 Defoliation outbreaks are biological disturbances that alter tree growth and mortality in

25 temperate forests. Trees respond to defoliation in many ways; some recover rapidly, while others

26 decline gradually or die. These differences may arise from species functional traits that constrain

27 growth such as xylem anatomy, growth phenology or non-structural carbohydrate (NSC) storage,

28 but this has not been shown. Although many studies address these phenomena, varied and

29 idiosyncratic measures limit our ability to generalize and predict defoliation responses across

30 species. I synthesized and translated published growth and mortality data into consistent

31 standardized variables suitable for numerical models. I analyzed data from 32 studies, including

32 16 tree species and 10 defoliator systems from North America and Eurasia, and quantitatively

33 compared responses to defoliation among species and tree functional groups using linear mixed-

34 effects models.

35 Relative growth decreased linearly or curvilinearly as defoliation stress accumulated across

36 species. Growth decreased by only 5-20% following 100% defoliation in ring-porous *Quercus*,

37 whereas growth of diffuse-porous hardwoods and conifers declined by 50-100%. Mortality

38 increased exponentially with defoliation, more rapidly for *Pinus* and diffuse-porous species than

39 for *Quercus* and *Abies*. Species-specific mixed models were best (R^2c = 0.83-0.94), yet

40 functional-group models lost little in terms of goodness-of-fit (R^2c = 0.72-0.92), providing useful

41 alternatives when species data is lacking. These responses are consistent with functional

42 differences in wood growth phenology and NSC storage. Ring-porous spring xylem growth

43 precedes budburst. Defoliators whose damage follows foliar development can only affect

44 development of later wood. Growth of diffuse-porous and coniferous species responds more

45 drastically, yet differences in NSC storage make them more vulnerable to mortality as stress

46 accumulates. Ring-porous species resist defoliation-related changes in growth and mortality

47   more than diffuse-porous and coniferous species. These findings apply in general to disturbances

48   that cause spring defoliation and should be incorporated into forest vegetation models.

49

50

Introduction

51

52   Tree and forest response to spring defoliation is a complex process. Trees lose photosynthetic

53   potential when they are defoliated early in the growing season, resulting in changes in growth.

54   They also die more often as defoliation stress interacts with other mortality factors. Yet trees are

55   long-lived, sessile organisms that must weather many disturbances over their lifetimes. In

56   adapting to this life history, they have become resilient to a wide range of climatic variation and

57   disturbance, including some amount of herbivory and defoliation. This adaptive resilience can

58   mask the effects of defoliation when disturbance years are observed in isolation, as some trees

59   show negligible response. Yet as stress accumulates over successive years of an outbreak,

60   changes in tree growth and mortality become more severe, consistent and interpretable

61   (MacLean 1980).

62   Tree responses to stress are increasingly viewed through the lens of inter-specific

63   differences in functional traits including leaf and wood growth phenology, xylem anatomy, and

64   non-structural carbohydrate (NSC) storage (Wiley & Helliker 2012, Panchen et al. 2014, Sevanto

65   et al. 2014). Ensembles of these traits are often linked. For example, deciduous species that leaf

66   out later tend to have larger xylem vessels than species that leaf out earlier (Lechowicz 1984,

67   Panchen et al. 2014), while species that store NSC primarily in leaves (conifers) tend to break

68   bud latest of all (Hoch et al. 2003, Michelot et al. 2012). These linkages may help explain

69   mechanisms of tree mortality under drought or other stresses (Sevanto et al. 2014), yet a

70   consensus on mortality mechanisms remains elusive (Wiley & Helliker 2012). Insect defoliation

71   is a periodic stressor of trees that is rarely brought to bear on ongoing discussions of carbon

72   starvation or hydraulic limitation hypotheses (Anderegg & Callaway 2012, Landhäusser &

73   Lieffers 2012). Yet defoliation stress is relatively straightforward: it directly limits the main

74 source of C during a critical growing period. A better understanding of functional differences in

75 tree response to defoliation would provide insight into responses to distinct climate-related

76 stresses such as drought or late frost.

77   Extensive research quantifies growth and mortality responses to defoliation, yet it

78 remains difficult to generalize the results across species and ecosystems due to the wide variety

79 of data, models, and scales used by individual studies (Feicht et al. 1993, Hallet et al. 2006).

80 These disparities present a significant obstacle to the development of general models that

81 simulate how defoliation affects forest productivity. While extensive reviews exist for general

82 (Kulman 1971) and species-specific defoliation effects (Davidson et al. 1999; Jacquet et al.

83 2012), they stop short of quantitatively synthesizing results to compare defoliator systems (but

84 see MacLean 1980). Comparisons are complicated by the common use of categorical measures

85 of defoliation that differ. These measures may be defined by quantitative limits (e.g. low,

86 medium, and high defoliation classes may correspond to 0-30%, 30-60%, 60-100% defoliation,

87 or other limits), but they are typically reported and discussed categorically. These limitations

88 leave a gap in our understanding about forest response to large-scale, recurring insect disturbance

89 that contributes significant uncertainty to landscape- and global vegetation models.

90   We can reduce uncertainty in forest models by quantifying the different ways species

91 respond to stress and how those responses are linked to functional traits. We can also improve

92 how observations from field-based studies are scaled to geographic extents that are compatible

93 with vegetation models. Recent innovations using satellite data to quantify and map defoliation

94 create the potential to link spatially accurate estimates of disturbance stress with forest

95 characteristics and response (Townsend et al. 2012, Foster et al. 2013). In order to improve forest

96 models with realistic representations of defoliation severity, we need numerical relationships that

97   link accumulated defoliation stress to growth suppression or mortality. Examples of such

98   empirical relationships exist for few defoliator systems (MacLean 1980; Alfaro et al. 1982). In

99   this analysis, I compare defoliation responses among several species from different tree

100   functional groups. I converted published data to standardized variables that lend themselves to

101   stand- and landscape-scale forest models and examined the data for significant trends,

102   relationships and differences among defoliator systems. Specifically, I sought studies that allow

103   quantification of both accumulated defoliation stress, which I define in a manner similar to

104   MacLean (1980) as the sum of annual defoliation over multiple years of an outbreak, and the

105   associated responses in terms of growth and mortality. I expected sensitivity to defoliation to

106   differ both by species and by functional groups defined by general tree-growth strategies.

107

108   **Materials and methods**

109   To test for generalizable relationships, I compiled research papers that reported defoliation as a

110   percentage of whole canopy foliage, or alternatively cumulative defoliation (defined as the sum

111   of annual defoliation over an outbreak or the product of average defoliation and outbreak

112   duration), as well as changes in growth and mortality as percentages (growth = % of average or

113   expected growth, cumulative mortality = % of population dying over a period of time, typically

114   5-10 years). Because repeated defoliation causes cumulative stress in trees, data from multiple

115   years of defoliation are of particular interest when modeling long-term effects (Blaise 1958;

116   MacLean 1980; Colbert & Fekedulegn 2001; Hennigar, MacLean & Norfolk 2007). Increasing

117   intensity over the duration of an outbreak can be captured by the summed, cumulative defoliation

118   in an objective, quantitative way (MacLean & Ostaff 1989). For papers where data were

119   presented in tables, graphs or text that could be converted to the described variables, I extracted,

120 transformed and analyzed them in a consistent manner. I assigned categorical annual or

121 cumulative defoliation values to the numerical midpoint of the reported defoliation range (e.g. a

122 150-300% cumulative defoliation category, became 225% defoliation) (MacLean & Lidstone

123 1982). I treated the spruce budworm system (SBW) (*Choristoneura fumiferana*) as a special case

124 because cumulative defoliation is defined uniquely in this literature as an index of defoliation by

125 foliage age-classes. To retain comparison with existing published relationships, I did not rescale

126 these data to fit my definition of cumulative "total" canopy defoliation (e.g. simultaneous

127 defoliation of all foliage age-classes).

128   I selected results that reported the aggregate response of all tree canopy classes when

129 available, as many forest models do not track individual trees or their canopy status (Mladenoff

130 2004). When data were only reported for separate canopy classes (i.e. suppressed, intermediate,

131 or dominant) and sample sizes were available, I used weighted averages of all classes to estimate

132 aggregate stand response (Campbell & Valentine 1972). I did not distinguish among differences

133 in growth or mortality variables, such as mortality expressed as a percentage of basal area (BA)

134 or number of stems. My goal was to determine if average trends could be found in the extensive

135 empirical literature and whether trends would vary among tree species groups. I expected

136 considerable variability in both the predictor and response variables across studies, as the

137 methods of their estimation often lacked precision. Many papers only reported means of

138 cumulative defoliation categories, and relationships fit to mean values mask the variability

139 present in the raw, unreported data. The R^2 values reported from mean-only data do not represent

140 the variability expected from plot-level data, which would presumably result in lower R^2.

141   I fit mortality response (%) to cumulative defoliation using a log transform to linearize

142 the relationship. I fit either linear or negative log-linear relationships between cumulative

143   defoliation and growth (%) where appropriate. I report parameters and results in tables and back-

144   transformed models in figures with the raw data. When possible, I also fit models to annual

145   mortality rates, calculated by dividing raw reported mortality by the number of years over which

146   it had accumulated. When multiple datasets for similar species or defoliator systems existed, I

147   used mixed models (nlme package in R) to create combined models for annual rates that varied

148   intercept and slope as random effects by study and compared the results using Akaike

149   information criterion for small sample sizes (AICc).

150

151   **Results**

152   *Growth Response*

153   Average radial growth decreased linearly with accumulated defoliation stress for 9 of 16 data

154   sets that reported usable data, and followed a negative exponential relationship for the remainder

155   (Table 1, Figs. 1 and 2). Cumulative defoliation explained from 17 to 99% of the variance in

156   relative growth depending on the dataset, with typical R^2 values exceeding 0.80 (Table 1). The

157   rate of growth suppression, i.e., the slope parameter, tended to vary bimodally. More sensitive

158   tree species-defoliator systems exhibited a negative slope equal to a 50-100% suppression in

159   growth for a 100% increase in cumulative defoliation (Fig. 2a) (Kulman, Hodson & Duncan

160   1963; Alfaro & Shepherd 1991; Gross 1992; Erdle & MacLean 1999), while growth of other

161   species was reduced by only 5-20% over the same defoliation range (Figs. 1, 2 and 3, Table 1,

162   Appendix S1 in Supporting Information) (Baker 1941; Rose 1958; Rubtsov 1996; Colbert &

163   Fekedulegn 2001; Naidoo & Lechowicz 2001). Conifers including *Abies balsamea*, *Pinus*

164   *banksiana, P. pinaster, P. sylvestrus*, *Psuedotsuga menziesii*, *Larix laricina*, and diffuse-porous

165   *Populus* and *Acer* species composed the more responsive group, showing immediate, strong

8

166   responses to a single year of defoliation. Species with slower, more moderate growth response

167   generated some radial growth even under severe defoliation, a trait characteristic of ring-porous

168   *Quercus* species, which have positive minimum growth thresholds due to their need to grow new

169   functional xylem cells every spring (Fig. 1). Trees with growth falling below these thresholds

170   would presumably reach a point from which they are unable to recover and subsequently leave

171   the pool of survivors. The lone deciduous conifer, *L. laricina*, responded less rapidly than *Pinus*

172   species, reducing growth at rates intermediate between examples of *P. tremuloides* and juvenile

173   *A. saccharum* (Appendix S1).

174   Negative curvilinear growth responses to defoliation were mostly associated with

175   immature trees (Fig. 2). These showed rapid early reductions in growth that were later

176   constrained by the theoretical minimum of zero (radial wood growth cannot be negative, though

177   stems will shrink under certain conditions (Stephens, Turner & Roo 1972; Wargo 1981; Alfaro et

178   al. 1982; Nichols 1988; Ostaff & Maclean 1995; MacLean & MacKinnon 1996)). The

179   curvilinear response is plausible in species that can survive many years without measurable

180   radial growth. Moreover, linear patterns become curvilinear if they approach lower bounds to

181   growth, and may simply represent a truncated view of the full relationship. This appears to be the

182   case for juvenile oaks that were manually defoliated by Wargo (1981) (Fig. 2a), whose growth

183   decreased more rapidly in a curvilinear fashion than mature, naturally defoliated oaks (Fig. 1).

184   Manually defoliated young *L. laricina* showed a similar curvilinear response (Fig. 2a). These

185   three patterns dominate the literature: negative curvilinear or linear growth responses with steep

186   or gradual slopes. This suggests consistent differences in the variability and range of growth

187   suppression among tree functional groups following defoliation stress.

188

9

189   *Mortality*

190   I derived standardized cumulative defoliation and mortality data for 12 published studies

191   covering broad areas of North American and Eurasian temperate forest, several tree species, and

192   seven distinct spring defoliators of hardwoods, conifers or both (Table 2). Mortality increased

193   exponentially in all examples, approaching a sigmoid curve if severe enough, or observed long

194   enough, to saturate at 100% (MacLean 1980). This pattern was first observed by Blaise (1958)

195   for *Abies balsamea* mortality following spruce budworm defoliation (Appendix S2). Though the

196   available data show a consistent form for mortality relationships, the parameters varied for

197   different tree species and defoliator systems (Fig. 3, Table 2, Appendix S2 and S3). Cumulative

198   defoliation explained 90% of the variation in cumulative mortality of *Quercus* dominated forests

199   following *Lymantria dispar* L. (gypsy moth (GM)) outbreaks (Table 2, Feicht et al. 1993).

200   Mortality increased slowly at first, until cumulative defoliation reached about 150%, after which

201   mortality increased rapidly, approaching 100% (Baker 1941; Campbell & Valentine 1972; Feicht

202   et al. 1993; MacLean & Ebert 1999). A similar exponential increase was observed for single year

203   defoliation levels less than or equal to 100% (Table 2, Dobbertin & Brang 2005).

204   Alfaro et al. (1982) used a powered exponential relationship to explain over 99% of the

205   variance in mortality of Douglas fir (*Pseudotsuga mensiesii*) following a *Choristoneura*

206   *occidentalis* (western spruce budworm (WSBW)) outbreak (Table 2, Appendix S2). This

207   relationship is very similar to one derived here for *Abies balsamea* (balsam fir) mortality

208   following *Choristoneura fumiferana* (eastern spruce budworm (SBW)) defoliation from two

209   separate studies (Table 2, Fig. 3) (Blais 1958; Batzer 1973). These data agree with anecdotal

210   reports of mortality becoming severe following 3-4 years of complete defoliation (Kulman

211   1971), though these systems take much longer than deciduous ones to reach an equivalent

212   amount of whole canopy defoliation (as opposed to defoliation of specific foliage age-classes

213   only). In particular, SBW outbreaks on *A. balsamea* take 10-12 years to produce equivalent

214   damage to entire canopies because they feed preferentially on current year foliage (MacLean

215   1980; MacLean & Ostaff 1989). Mortality in *A. balsamea* following *Lambdina fiscellaria*

216   *fiscellaria* (hemlock looper), a defoliator of all foliage age-classes, led to a more rapid increase

217   in mortality, closer to the range observed for *Pinus* species (Table 2, Appendix S2) (MacLean &

218   Ebert 1999).

219   When data from three studies of *Pinus* response, including mortality of young *P. strobus*

220   following GM defoliation and mature *P. banksiana* following *Choristoneura pinus pinus* (jack

221   pine budworm (JPBW)) defoliation (Baker 1941; Kulman et al. 1963) were combined (Fig. 3),

222   the best fit model shows mortality increasing more rapidly for defoliated *Pinus* than *Quercus*

223   species (Fig. 3, Appendix S2 and S3). Pines are typically thought to be capable of withstanding

224   only a few years of complete or severe defoliation, consistent with this rapid increase in

225   mortality (O'Neil 1962; Volney 1998).

226

227   *Differences in response models: species vs. functional group*

228   For cases where it was possible to formally compare mixed models (Appendix S3), models with

229   species-specific parameters always ranked higher than models that varied random effects based

230   on functional group. Species-specific random effects were best for all response models

231   regardless of whether intercepts, slopes, or both were varied (Appendix S3). Though species-

232   specific models represented the data best, functional group models lost little in terms of

233   goodness-of-fit. The variance explained by the best curvilinear growth response model by

234   functional group ($R^2c = 0.72$) was not much lower than variance explained by the best species

235   model (R^2c=0.83) (Appendix S3) (Nakagawa & Schielzeth 2013). Variance explained by the best

236   linear growth response models was similarly high for functional group (R^2c=0.92) as for species

237   (R^2c=0.94), and the best mortality functional group model (R^2c=0.82) lost little predictive power

238   compared to the best species model (R^2c=0.87). The similar predictive power of species and

239   functional group models suggests that functional group can be used as a surrogate to predict

240   growth and mortality response for tree species that lack data. It should be noted that mixed

241   models that vary only intercepts (*Quercus*, *Pinus*, Appendix S3) may be detecting differences

242   among the methods used by different studies to relativize growth responses against "normal"

243   growth, rather than meaningful biological differences among species.

244

245   **Discussion**

246   *Relationship of growth and mortality responses to phenology, wood anatomy and NSC storage*

247   Differences in growth strategies and wood anatomy among tree functional groups may help

248   explain the observed differences in shape and slope of the relationships reported here. For

249   example, oaks that survive several years of gypsy moth defoliation show a linear reduction in

250   growth of about 14-17% per 100% increase in defoliation. The best mixed models showed that

251   slopes did not differ significantly for analogous data collected in New England, Quebec, and

252   Russia (Baker 1941; Rubtsov 1996; Naidoo & Lechowicz 2001) (Appendix S3). Over the course

253   of an outbreak, radial growth was reduced by an average of 50-60% in these examples, but rarely

254   more. Temperate oaks are ring-porous species that must rely on large early wood vessels for

255   hydraulic transport. More than 90% of these vessels cavitate under freezing winter temperatures,

256   meaning that oaks' hydraulic architecture will not function from one year to the next (Sperry et

257   al. 1994; Davis, Sperry & Hacke 1999). Temperate oaks overcome this limitation by storing

258   excess starch reserves in sapwood over winter and drawing on them to build new xylem elements

259   the following spring (Barbaroux & Breda 2002). This early wood radial growth will actually

260   precede flushing of the leaves by two to six weeks, and is necessary to supply water to

261   developing foliage (Lechowicz 1984; Hacke & Sauter 1996; Suzuki, Yoda & Suzuki 1996,

262   Michelot et al. 2012). Accordingly, many *Quercus* species, and large vessel ring-porous species

263   in general, leaf-out later than other deciduous species (Lechowicz 1984, Panchen et al. 2014).

264   Growth phenology research using dendrometer bands has documented examples where 30% of

265   radial growth is completed before budburst, and 40% by the time tree canopies achieve

266   maximum LAI in June (Kulman et al. 1963; Hinckley & Lassoie 1981; Barbaroux & Breda

267   2002, Zweifel et al. 2006). Similarly, 50% of the total annual xylem was formed by June for

268   *Fraxinus excelsior*, another ring-porous species (Ladefoged 1952). As a consequence of these

269   traits, by the time larvae of spring defoliators are large enough to cause severe defoliation

270   damage, many oaks have already completed 30-40% of annual radial growth in the form of early

271   wood (Kozlowski 1969, Zweifel et al. 2006).

272   Xylem vessels are necessary for conductance to support leaves and photosynthesis,

273   creating a minimum cambial growth threshold for temperate, deciduous oaks that is typically 20-

274   40% of average radial growth. The curvilinear growth response of juvenile *Quercus* trees

275   defoliated by Wargo (1981) illustrates this well (Fig, 2a). Trees that are depleted of starch and

276   unable to regenerate a minimum vessel layer the following spring are likely to die and leave the

277   survivor pool. Studies of non-structural carbohydrate (NSC) storage also support this hypothesis,

278   though the mechanisms of the carbon starvation hypothesis remain in question (Hoch, Richter &

279   Korner 2003; Landhäusser & Lieffers 2012). Hoch et al. (2003) measured NSC allocation and

280   reserves for seven deciduous and three evergreen tree species and estimated that typical C

281   reserves in deciduous species could regenerate the equivalent of four canopies of foliage. This

282   estimate agrees with anecdotal evidence that many trees die following three to four years of

283   complete defoliation and is consistent with curvilinear mortality rates (Fig. 3, Appendix S2).

284   Wargo (1981) measured starch reserves in juvenile *Q. velutina* and *Q. alba* as well as *Acer*

285   *saccharum* following three years of 100% artificial defoliation of June foliage. Starch dropped

286   curvilinearly to 11% and 0.2 % of average in *Q. alba* and *Q. velutina*, respectively. Starch in *A.*

287   *saccharum* dropped to 0%, leading to complete mortality. Diffuse-porous species such as *A.*

288   *saccharum* are less sensitive to limited radial growth. They retain multiple rings of functioning

289   xylem to meet hydraulic requirements. They may be more sensitive to rapid reductions in starch,

290   as they are less thrifty with NSC storage than *Quercus* species (Wargo 1981; Barbaroux & Breda

291   2002).

292   Diffuse-porous tree species from genera such as *Populus* (aspen), *Acer* (maples), and

293   *Fagus* (beech) demonstrate a different growth phenology than oaks. This phenology could

294   explain their wider range of radial growth response to defoliation. The smaller vessels in diffuse-

295   porous wood rarely cavitate and water transport is thus possible using existing xylem as soon as

296   spring conditions are suitable for budburst and shoot elongation (Lechowicz 1984; Davis et al.

297   1999). Diffuse-porous species typically utilize multiple annual rings for proper hydraulic

298   function. As a result, diffuse-porous species store less starch in sapwood, only needing enough to

299   generate a new set of foliage. These species leaf-out as early as possible when growing

300   conditions become suitable for early leaf development (Panchen et al. 2014), and the probability

301   of late frosts decreases (Barbaroux & Breda 2002). Diffuse-porous wood anatomy is often linked

302   to indeterminate growth habits, which allow species to continue to grow and respond to changing

303   conditions throughout the growing season (Kozlowski 1992). In comparison to ring-porous

14

304   *Quercus*, diffuse-porous *Fagus* leaf-out earlier in the spring, do not initiate measurable radial

305   growth until two to seven weeks after budburst has occurred, and may achieve only 5-10% of

306   annual growth by the time canopies reach maximum LAI (Suzuki et al. 1996; Schmitt, Moller &

307   Eckstein 2000; Barbaroux & Breda 2002, Michelot et al. 2012)). In such cases, June herbivory

308   by defoliator larvae could suppress radial growth by up to 95%. The wider range in growth

309   response of diffuse-porous species leads to a steeper negative slope as defoliation stress

310   accumulates. At the same time, these strategies may improve survivability for some diffuse-

311   porous species, such as *Populus tremuloides*, by allowing trees to dedicate more available

312   photosynthate and NSC reserves to refoliation or chemical defense, rather than replenishing

313   reserves for future spring wood growth. The empirical evidence in the literature remains

314   equivocal on this topic. This review shows that defoliated young *A. saccharum* and mature *P.*

315   *tremuloides* do demonstrate a wider range in radial growth suppression than *Quercus* species

316   (Fig. 2); their growth was suppressed to below 20% of average over the observed range of

317   defoliation.

318   Conifers that retain foliage for multiple years employ yet another growth strategy that

319   contributes to a wider dynamic range of response to cumulative defoliation stress. Conifers that

320   retain two to three years of foliage (most *Pinus*) respond differently from those that retain four to

321   eight years of foliage age-classes (*Abies, Pseudotsuga*), as pines are generally more vulnerable to

322   their defoliators than firs. Conductive tissue in coniferous stemwood is made up of tracheids that

323   resist cavitation, a necessity for retention of green leaves throughout the winter dormant season

324   (Hinckley & Lassoie 1981; Tyree & Ewers 1991). Like diffuse-porous species, conifers are not

325   dependent on radial growth to renew xylem function and can survive periods with no radial

326   growth. This characteristic shows up as dropped rings in dendrochronological research. Unlike

15

327   deciduous trees, conifers tend to utilize older foliage more than sapwood for NSC storage, and

328   rely on translocation from those stores to grow new foliage in the spring (Kozlowski 1992; Hoch

329   et al. 2003). New, current-year foliage is also responsible for a greater proportion of net

330   photosynthate production than older foliage. These characteristics mean radial growth response

331   to defoliation can range from 0-100%, and variation in preferential herbivory of old or new

332   foliage can produce linear or nonlinear relationships (Fig. 2b).

333   The simple, general relationships compiled here indicate that increasing defoliation stress

334   slows carbon accumulation in host species through destruction of foliar biomass and suppression

335   of radial stem growth. Productivity can be slowed at different rates, depending on the plasticity

336   and phenology of tree growth response and defoliator characteristics. Continuous defoliation also

337   increases tree mortality exponentially. Mortality rates increase most rapidly in *Pinus*, followed

338   by diffuse-porous genera such as *Acer* and *Populus*, then *Quercus*, and more slowly in *Abies* and

339   *Pseudotsuga* whose pests exhibit different feeding behavior. Nonlinear growth and mortality

340   responses can lead to extreme short-term losses in aboveground carbon. These relationships

341   allow us to more accurately quantify and model landscape-level effects on forest carbon

342   accumulation. This framework and approach for quantifying the accumulation of defoliation

343   stress and associated growth and mortality responses can be used in future empirical research to

344   facilitate comparison across more defoliator systems.

345

346   **Acknowledgements**

349   guidance, support and editorial review, as well as B. Sturtevant, K. Raffa, M. Turner, P.

350   Townsend, D. Lorimer, and A. Pessin for comments on early versions of this manuscript.

351

352   **Data Accessibility**

353   -   Defoliation, growth and mortality data extracted and transformed from published studies

354   will be archived on DRYAD, as well as associated R-scripts allowing replication of the

355   analysis.

356   -   Appendix S1. Plots of derived growth data and back-transformed model fits by study:

357   uploaded as online supporting information

358   -   Appendix S2. Plots of derived mortality data and back-transformed model fits by study:

359   uploaded as online supporting information

360   -   Appendix S3. Model selection and parameter fits for mixed models of growth and

361   mortality data that could be compared within defoliator systems or across species groups:

362   uploaded as online supporting information

363

364   **References**

365   Alfaro RI, Shepherd RF (1991) Tree-ring growth of interior douglas-fir after one year defoliation

366   by douglas-fir tussock moth. For Sci 37:959-964.

367   Alfaro RI, Vansickle GA, Thomson AJ, Wegwitz E (1982) Tree mortality and radial growth

368   losses caused by the western spruce budworm in a douglas-fir stand in British Columbia. Can J

369   For Res 12:780-787.

370 Anderegg WRL, Callaway ES (2012) Infestation and hydraulic consequences of induced carbon

371   starvation. Plant Physiology 159:1866-1874.

372 Baker WL (1941) Effect of gypsy moth defoliation on certain forest trees. J For 39:1017-1022.

373 Barbaroux C, Breda N (2002) Constrasting distribution and seasonal dynamics of carbohydrate

374   reserves in stem wood of adult ring-porous sessile oak and diffuse-porous beech trees. Tree

375   Physiol 22:1201-1210.

376 Batzer HO (1973) Net effect of spruce budworm defoliation on mortality and growth of balsam

377   fir. J For 71:34-37.

378 Blaise JR (1958) The vulnerability of balsam fir to spruce budworm attack in northern Ontario,

379   with special reference to physiological age of the tree. For Chron 34:405-422.

380 Campbell RW, Valentine HT (1972) Tree condition and mortality following defoliation by the

381   gypsy moth. U.S. Department of Agriculture, Forest Service, Northeastern Forest Experiment

382   Station, Upper Darby, PA, Res. Pap. NE-236.

383 Churchill GB, John HH, Duncan DP, Hodson AC (1964) Long-term effects of defoliation on

384   aspen by the forest tent caterpillar. Ecology 45:630-636.

385 Colbert JJ, Fekedulegn D (2001) Effects of gypsy moth defoliation on tree growth - preliminary

386   models for effects of cumulative defoliation on individual host tree radial increment.

387 Proceedings: integrated management and dynamics of forest defoliating insects, Victoria, BC.,

388 U.S. Department of Agriculture, Forest Service, Northeastern Research Station

389   Davidson CB, Gottschalk KW, Johnson JE (1999) Tree mortality following defoliation by the

390   European gypsy moth (L*ymantria dispar* L.) in the United States: a review. For Sci 45:74-84.

391   Davis SD, Sperry JS, Hacke UG (1999) The relationship between xylem conduit diameter and

392   cavitation caused by freezing. A J Bot 86:1367-1372.

393   Dobesberger EJ (1998) Stochastic simulation of growth loss in thinned balsam fir stands

394   defoliated by the spruce budworm in Newfoundland. Can J For Res 28:703-710.

395   Feicht DL, Sandra LC (1993) Forest stand conditions after 13 years of gypsy moth infestation.

396   Proceedings of the 9th Central Hardwood Forest Conference; Gen. Tech. Rep. NC-161, St. Paul,

397   MN, U.S. Department of Agriculture, Forest Service, North Central Forest Experiment Station.

398   Foster JR, Townsend PA, DJ Mladenoff (2013). Spatial dynamics of a gypsy moth defoliation

399   outbreak and dependence on habitat characteristics. Landscape Ecol 28:1307-1320.

400   Gross HL (1992) Impact analysis for a jack pine budworm infestation in Ontario. Can J For Res

401   22:818-831.

402   Hacke U, Sauter JJ (1996) Xylem dysfunction during winter and recovery of hydraulic

403   conductivity in diffuse-porous and ring-porous trees. Oecologia 105:435-439

404   Hallett RA, Bailey SW, Horsley SB, Long RP (2006) Influence of nutrition and stress on sugar

405   maple at a regional scale. Can J For Res 36:2235-2246.

406   Hennigar CR, MacLean DA, Norfolk CJ (2007) Effects of gypsy moth defoliation on softwood

407   and hardwood growth and mortality in New Brunswick, Canada. Northern J Appl For 24:138-

408   145.

409   Herrick OW, Gansner DA (1987) Gypsy moth on a new frontier: forest tree defoliation and

410   mortality. Northern J Appl For 4:128-133.

411   Hinckley TM, Lassoie JP (1981) Radial growth in conifers and deciduous trees: a comparison.

412   Mitteilungen der Forstlichen Bundes Versuchsanstalt Wien 142:17-56

413   Hoch G, Richter A, Korner C (2003) Non-structural carbon compounds in temperate forest trees.

414   Plant Cell Environ 26:1067-1081.

415   Ives WG, Nairn LD (1966) Effects of defoliation on young upland tamarack in Mantioba. For

416   Chron 42:137-142.

417   Jacquet J, Orazio C, Jactel H (2012) Defoliation by processionary moth significantly reduces tree

418   growth: a quantitative review. Ann For Sci 69:857-866.

419   Jacquet J, Bosc A, O'Grady AP, Jactel H (2013) Pine growth response to processionary moth

420   defoliation across a 40-year chronosequence. For Ecol Manage 293:29-38.

421   Kozlowski TT (1969) Tree physiology and forest pests. J For 67:118-123.

422   Kozlowski TT (1992) Carbohydrate sources and sinks in woody plants. Bot Rev 58:107-222.

423   Kulman HM, Hodson AC, Duncan DP (1963) For Sci 9:146-157.

424   Kulman HM (1971) Effects of insect defoliation on growth and mortality of trees. Annu Rev

425   Entomol 16:289-324.

426   Ladefoged K (1952) The periodicity of wood formation. Danske Videnskabernes Selskab.

427   Biologiske skrifter. bd. 7. no. 3. København : Ejnar Munksgaard.

428   Landhaeusser SM, Lieffers VJ (2012) Defoliation increases risk of carbon starvation in root

429   systems of mature aspen. Trees Struc Func 26:653-661.

430   Lechowicz MJ (1984) Why do temperate deciduous trees leaf out at different times – adaptation

431   and ecology of forest communities. Am Nat 124:821-842.

432   Landhäusser SM, Lieffers VJ (2012) Defoliation increases risk of carbon starvation in root

433   systems of mature aspen. Trees 26:653-661.

434   Lyytikainen-Saarenmaa P, Tomppo E (2002) Impact of sawfly defoliation on growth of Scots

435   pine *Pinus sylvestris* (Pinaceae) and associated economic losses. Bull Entomol Res 92:137-140.

436   MacLean DA (1980) Vulnerability of spruce stands during uncontrolled spruce budworm

437   outbreaks – a review and discussion. For Chron 56:213-221.

438   MacLean DA, Ebert P (1999) The impact of hemlock looper (*Lambdina fiscerllaria fiscellaria*

439   (Guen.)) on balsam fir and spruce in New Brunswick, Canada. For Ecol Manage 120:77-87.

440   MacLean DA, Lidstone RG (1982) Defoliation by spruce budworm: estimation by ocular and

441   shoot-count methods and variability among branches, trees, and stands. Can J For Res 12:582-

442   594.

443   MacLean DA, MacKinnon WE (1996) Accuracy of aerial sketch-mapping estimates of spruce

444   budworm defoliation in New Brunswick. Can J For Res 26:2099-2108.

445   MacLean DA, Ostaff DP (1989) Patterns of balsam fir mortality caused by an uncontrolled

446   spruce budworm outbreak. Can J For Res 19:1087-1095.

447   Man R, Kayahara GJ, Rice JA, MacDonald GB (2008) Response of trembling aspen to partial

448   cutting and subsequent forest tent caterpillar defoliation in a boreal mixedwood stand in

449   northeaster Ontario, Canada. Can J For Res 38:1349-1356.

450   Michelot A, Simard S, Rathgeber C, Dufrene E, Damesin C (2012) Comparing the intra-annual

451   wood formation of three European species (*Fagus sylvatica, Quercus petraea* and *Pinus*

452   *sylvestris*) as related to leaf phenology and non-structural carbohydrate dynamics. Tree Phys 32:

453   1033-1043.

454   Mladenoff DJ (2004) LANDIS and forest landscape models. Ecol Modell 180:7-19.

455   Naidoo R, Lechowicz MJ (2001) Effects of gypsy moth on radial growth of deciduous trees. For

456   Sci 47:338-348.

457   Nakagawa S, Schielzeth H (2013) A general and simple method for obtaining R^2 from

458   generalized linear mixed-effects models. Method Ecol Evol 4:133-142.

459   O'Neil LC (1962) Some effects of artificial defoliation on the growth of jack pine (*Pinus*

460   *banksiana* Lamb.). Can J Bot 40:273-280.

461   Ostaff DP, Maclean DA (1995) Patterns of balsam fir foliar production and growth in relation to

462   defoliation by spruce budworm. Can J For Res 25:1128-1136.

463   Panchen ZA, Primack RB, Nordt B, Ellwood ER, Stevens A, Renner SS, Willis CG, Fahey R,

464   Whittemore A, Du Y, Davis CC (2014) Leaf out times of temperate woody plants are related to

465   phylogeny, deciduousness, growth habit and wood anatomy. New Phytol 203:1208-1219.

466   Reichenbacker RR, Schultz RC, Hart ER (1996) Artificial defoliation effect on *Populus* growth,

467   biomass production, and total nonstructural carbohydrate concentration. Popul Ecol 25:632-642.

468   Rose AH (1958) The effect of defoliation on foliage production and radial growth of quaking

469   aspen. For Sci 4:335-342.

470   Salemaa M, Jukola-Sulonen E (1990) Vitality rating of *Picea abies* by defoliation class and other

471   vigour indicators. Scand J Forest Res 5:413-426.

472   Simmons MJ, Lee TD, Ducey MJ, Elkinton JS, Boettner GH, Dodds KJ (2014) Effects of

473   invasive winter moth defoliation on tree radial growth in eastern Massachusetts, USA. Insects

474   5:301-318.

475   Schmitt U, Moller R, Eckstein D (2000) Seasonal wood formation dynamics of beech (*Fagus*

476   *sylvatica* L.) and black locust (*Robinia pseudoacacia* L.) as determined by the "pinning"

477   technique. J Appl Bot-Angew Bot 74:10-16.

478   Sevanto S, McDowell NG, Dickman LT, Pangle R, Pockman WT (2014) How do trees die? A

479   test of the hydraulic failure and carbon starvation hypotheses. Plant Cell Environ 37:153-161.

480   Sperry JS, Nichols KL, Sullivan JEM, Eastlack SE (1994) Xylem embolism in ring-porous,

481   diffuse-porous, and coniferous trees of northern Utah and interior Alaska. Ecology 75:1736-

482   1752.

483   Stephens GR, Turner NC, De Roo HC (1972) Notes: Some effects of defoliation by gypsy moth

484   (*Porthetria dispar* L.) and elm spanworm (*Ennomos subsignarius* Hbn.) on water balance and

485   growth of deciduous forest trees. For Sci 18:326-330.

486   Suzuki M, Yoda K, Suzuki H (1996) Phenological comparison of the onset of vessel formation

487   between ring-porous and diffuse-porous deciduous trees in a Japanese temperate forest. Iawa

488   J17:431-444.

489   Townsend PA, Singh A, Foster JR et al (2012) A general Landsat model to predict canopy

490   defoliation in broadleaf deciduous forests. Remote Sens Environ 119: 225-265.

491   Tyree MT, Ewers FW (1991) The hydraulic architecture of trees and other woody-plants. New

492   Phytol 119:345-360.

493   Volney WJA (1998) Ten-year tree mortality following a jack pine outbreak in Saskatchewan.

494   Can J For Res 28:1784-1793.

495   Wiley E, Helliker B (2012) A re-evaluation of carbon storage in trees lends greater support for

496   carbon limitation to growth. New Phytol 195:285-289.

497   Williams DT, Straw NA, Day KR (2003) Defoliation of Sitka spruce by the European spruce

498   sawfly, *Gilpinia hercyniae* (Hartig): a retrospective analysis using the needle trace method. Agr

499   Forest Entomol 5:235-245.

500   Zweifel R, Zimmermann L, Zeugin F, Newbery DM (2006) Intra-annual radial growth and water

501   relations of trees: implications towards a growth mechanism. J Exp Botany 57:1445-1459.

502

503

504   **Figure Legends**

505

506   **Figure 1.** Growth response of *Quercus* species to *Lymantria dispar* (L.) (gypsy moth) defoliation

507   including *Quercus robur* (Rubstov 1996), *Q. velutina* (Baker 1941), *Q. rubra* (Wargo 1981), and

508   *Quercus alba* (Baker 1941, Wargo 1981). Lines show best fit mixed model (Appendix S3, Table

509   S3-1). The best combined *Quercus* model varied intercepts but not slopes.

510

511   **Figure 2.** Growth decreases curvilinearly to defoliation (a.) in *Populus tremuloides* (Rose 1958),

512   manually defoliated juvenile trees of *Acer saccharum*, *Q. alba*, and *Q. velutina* (Wargo 1981),

513   and *Larix laricina* (Ives and Nairn 1966). Linear growth responses of coniferous species (b.)

514   include steep declines in *Pinus banksiana*, *P. pinaster*, *P. sylvestrus* with slower declines in

515   *Pseudotsuga menziesii, Picea abies,* and *Abies balsamea*. The best fit mixed model (a., lines)

516   randomly varied slopes but not intercepts (Appendix S3, Table S3-1). Lines in (b.) show model

517   fits from Table 1 and the best mixed model for *Pinus* species that varied intercept, but not slope

518   (Appendix). *A. balsamea* relationship was published by Dobesberger 1998.

519

520   **Figure 3.** Cumulative mortality responses of example tree species to accumulated defoliation.

521   Mortality rates rise most quickly in *Pinus* (Baker 1941, Kulman et al. 1963, Gross 1992),

522   followed by diffuse-porous *Populus* (Mann et al. 2007), and then ring-porous *Quercus*

523   dominated forests (Feicht et al. 1993). Mortality in *Abies* appears to rise more slowly (Blais

524   1958, Batzer 1973), but defoliation in this system is defined differently as damage by foliage

525   age-class. Lines show model fits from Table 2. All plots can be found in Appendix S2.

526

527

25

528 **Table 1.** Models of relative tree growth response to cumulative defoliation. Input data were extracted and relativized from original
529 studies to the same scale (details below).
530

Location	Cum Defo.† Range (%)	Growth* Var. (%)	Equation	b	m	R^2	Reference
Lymantria dispar (L.) defoliation of *Quercus robur*							
Russia	0-300	RW	$y=mx+b$	80.00	-0.141	0.443	Rubstov (1996), Fig. 3
Lymantria dispar (L.) defoliation of *Q. coccinea, Q. alba,* and *Q. velutina*							
Maine Massachusetts	0-400	Radial inc.	$y=mx+b$	96.177	-0.110	0.437	Baker (1941), Table 5
New England	0-800	Radial inc.	$y=mx+b$	70.553	-0.039	0.935	Baker (1941), Table 4
Lymantria dispar (L.) defoliation of *Q. alba,* and *Q. rubra*							
New England	0-185	RW	$y=mx+b$	95.674	-0.278	0.877	Wargo (1981), Table 5.3
N. Temperate	0-800	all	$y=mx+b$	78.981	-0.100	0.254	Combined above
Quebec	NA	RW	$y=mx+b$	83.2	-0.165	0.730	Naidoo & Lechowicz (2001), Figure 6‡
Pennsylvania	0-170	RW index	$y=mx+b$	99.75	-0.168	0.168	Colbert & Fekedulegn (2001), Fig. 10‡
Operophtera brumata L.defoliation of *Q. rubra* and *Q. velutina*							
Massachusetts	0-100	RW index	$y=mx+b$	120.2	-0.60	0.24	Simmons et al. (2014), Fig. 2‡

Location	Cum. Defo.† Range (%)	Growth* Var. (%)	Equation	b	m	R^2	Reference
Malacosoma disstria (Hubn.) defoliation of *Populus tremuloides*							
Ontario	0-100	Radial inc.	$y=be^{mx}$	4.346	-0.006¶	0.470	Rose (1958), Fig. 4
Manual defoliation of juvenile *Populus deltoides* clones							
Iowa	0-75	AGB inc.	$y=mx+b$	103.38	-0.442	0.613	Reichenbacker et al. (1996), Table 3
Manual defoliation of immature *Acer Saccharum*							
Eastern US	0-300	Radial inc.	$y=be^{mx}$	4.677	-0.015	0.984	Wargo (1981), Table 5-10c
Manual defoliation of immature *Quercus alba*							
Eastern US	0-300	Radial inc.	$y=be^{mx}$	4.572	-0.005	0.995	Wargo (1981), Table 5-10b
Manual defoliation of immature *Quercus velutina*							
Eastern US	0-300	Radial inc.	$y=be^{mx}$	4.382	-0.004 §	0.791	Wargo (1981), Table 5-10a
Choristoneura pinus pinus (Free) on *Pinus banksiana*							
N. America	0-94	Summerwood	$y=mx+b$	79.323	-0.826	0.998	Kulman et al. (1963), Table 4
Thaumetopoea pityocampa (Dennis & Schiff) defoliation of *Pinus pinaster* Ait.							
France	0-100	Radial inc.	$y=mx+b$	95.604	-0.874	0.983	Jacquet et al. (2013), Fig. 1
Diprion pini (Linneaus) defoliation on *Pinus sylvestrus*							

594

595 Finland   0-100   RW $y=be^{mx}$ 4.328 -0.029¶ 0.975 Lyytkainen-Saarenmaa et al. (2002), Fig. 2

596

597 N. Temperate 0-100 all $y=mx+b$ 82.666 -0.829 0.853 *Pinus* above combined

598

599 *Orgyia pseudotsugata* (McDunnough) defoliation of *Psuedotsuga menziesii*

600

601 British   0-81   RW index $y=mx+b$ 88.080 -0.575 0.829 Alfaro & Shepherd (1991), Table 1
602 Columbia

603

604 *Choristoneura fumiferana* defoliation on *Abies balsamea*

605

606 Newfoundland 0-100 Volume inc. $y=mx+b$ 100   -0.63 0.950 Dobesberger (1998), Equation 9‡

607

608 General defoliation on *Picea abies*

609

610 Finland   0-100   Volume inc. $y=mx+b$ 116.31 -1.019 0.579 Salemaa & Jukola-Sulonen (1990), Fig. 3b

611

612 *Gilpinia hercyniae* (Hartig) defoliation on *Picea sitchensis*

613

614 Wales   0-70   Volume inc. $y=mx+b$ 92.39 -0.600 0.570 Williams (2003), Tables 2 & 3

615

616 Manual defoliation of young *Larix laricina*

617

618 Manitoba 0-300 Volume inc. $y=be^{mx}$ 5.146 -0.010 0.800 Ives & Nairn (1966), Fig. 1

619 * Growth is scaled from 0-100% of expected growth, either modeled, derived or observed in a control or prior to disturbance. Growth
620 was measured by ring widths (RW), RW index, radial increment, volume increment, or summerwood width or some derivation of
621 these. Please consult original articles for details.
622 † Cumulative defoliation is the sum of annual defoliation (0-100%) over the duration of a single outbreak (typically 1-5+ years).
623 ‡ Relationships published by original authors, included for comparison. When possible, formulae were rescaled to standardized ranges
624 used here.
625 ¶ Probability that parameter is different from zero between 0.05 and 0.10. Probability of unmarked parameters < 0.05.
626 § Probability that parameter is different from zero > 0.10.

627 **Table 2.** Models of cumulative tree mortality or annual mortality rates derived from cumulative defoliation.
628

Location	Cum Defo. Range (%)	Mort. Var. (%)	Annual Rate	Equation	b	m	R^2	Reference
Lymantria dispar (L.) defoliation of all species, *Quercus* dominant								
Pennsylvania	0-365	BA		$y=e^{(mx+b)}$	1.704	0.008	0.901	Feicht et al. (1993), Table 2 & 3
			yes	$(y+1)=e^{(mx+b)}$	0.521	0.006	0.876	Feicht et al. (1993), Table 2 & 3
New England	0-263	stems		$y=e^{(mx+b)}$	1.495	0.010	0.574	Campbell & Valentine (1972), Tables 1,2,227-233
			yes	$(y+1)=e^{(mx+b)}$	0.415§	0.007	0.662	Campbell & Valentine (1972), Tables 1,2,227-233
New England	0-80	stems	yes	$y=e^{(mx+b)}$	1.611	0.010	0.773	Baker (1941), Table 1
Pennsylvania	0-210	stems		$y=e^{(mx+b)}$	2.145	0.005	0.993	Herrick & Gansner (1987)
			yes	$y=e^{(mx+b)}$	0.535	0.005	0.993	Herrick & Gansner (1987)
N. America	0-365	all	yes	$(y+1)=e^{(mx+b)}$	0.547	0.006	0.839	Combined above, excluding Baker (1941)
Malacosoma disstria (Hubn.) defoliation of *Populus tremuloides*								
Ontario	0-300	stems		$y=e^{(mx+b)}$	2.135	0.008	0.918	Man et al. (2008), Fig. 4 & Table 1
			yes	$y=e^{(mx+b)}$	0.583	0.007	0.981	Man et al. (2008), Fig. 4 & Table 1
Minnesota	0-350	stems	yes	$(y+1)=e^{(mx+b)}$	2.806	0.007	0.667	Churchill et al. (1964), Table 1 and Text
General defoliation of *Acer Saccharum*								
N. America	0-95	BA	yes	$y=e^{(mx+b)}$	-0.784	0.045§	0.851§	Hallett et al. (2006), Fig. 4

Location	Cum Defo. Range (%)	Mort. Var. (%)	Annual Rate	Equation	b	m	R^2	Reference
Lymantria dispar (L.) defoliation on *Acer rubrum*								
New England	0-263	stems		$y= e^{(mx+b)}$	2.202	0.006¶	0.457	Campbell & Valentine (1972), Tables 183-189
			yes	$y= e^{(mx+b)}$	0.155§	0.007	0.612	Campbell & Valentine (1972), Tables 183-189
Lymantria dispar (L.) defoliation on *Pinus strobus*								
New England	0-100	stems		$(y+1)= e^{(mx+b)}$	1.207§	0.018§	0.314	Baker (1941), Table 3
			yes	$(y+1)= e^{(mx+b)}$	0.205§	0.009	0.516	Baker (1941), Table 3
Choristoneura pinus pinus (Free) on *Pinus banksiana* combined with above								
N. America	0-138	stems		$(y+1)= e^{(mx+b)}$	1.552	0.014	0.418	Baker (1941), Kulman et al. (1963), Gross (1992)
			Yes	$(y+1)= e^{(mx+b)}$	0.429§	0.012	0.505	Baker (1941), Kulman et al. (1963), Gross (1992)
Choristoneura occidentalis (Freeman) defoliation of *Psuedotsuga menziesii*								
British Columbia	150-400	stems		$y= e^{(mx+b)}$	-1.163§	0.016	0.955	Alfaro et al. (1982), Fig. 6
			yes	$(y+1)= e^{(mx+b)}$	-3.424	0.016	0.955	
Lambdina fiscellaria fiscellaria (Guen.) defoliation on *Abies balsamea*								
New Brunswick	0-100	stems	yes	$y= e^{(mx+b)}$	-0.311§	0.040	0.830	MacLean & Ebert (1999), Fig. 4
	0-400	stems		$y=10^{(mx+b)}$	0.647	0.006	0.790	MacLean & Ebert (1999), Fig. 6 ‡
		volume	yes	$y=10^{(mx+b)}$	0.647	0.006	0.817	MacLean & Ebert (1999), Fig. 6 ‡
Choristoneura fumiferana defoliation on *Abies balsamea*								
Ontario	0-400	stems		$(y+1)= e^{(mx+b)}$	-0.642	0.013	0.950	Blaise (1958), Fig. 2 & Table 1
			yes	$(y+1)= e^{(mx+b)}$	-0.445	0.006	0.890	Blaise (1958), Fig. 2 & Table 1

693
694 Minnesota   150-475 BA $(y+1)= e^{(mx+b)}$ 0.891§ 0.007 0.847 Batzer (1973), Fig. 1
695   yes $(y+1)= e^{(mx+b)}$ -0.23 § 0.006 0.831 Batzer (1973), Fig. 1
696
697 N. America 0-475   all $(y+1)= e^{(mx+b)}$ -0.352§0.011 0.914 Batzer (1973), Blaise (1958)
698   yes $(y+1)= e^{(mx+b)}$ -0.417 0.006 0.900 Batzer (1973), Blaise (1958)
699
700 All defoliation, all species
701
702 Switzerland 0-100   stems   yes $y= e^{(mx+b)}$ -3.050 0.062 0.924 Dobbertin and Brang (2001), Fig. 1
703
---
704 * Mortality ranges from 0-100% of the live tree population expressed as number of stems, basal area (BA), or volume.
705 † Cumulative defoliation is the sum of defoliation (0-100%) over the duration of a single outbreak.
706 ‡ Relationships published by original authors, included for comparison. When possible, formulae were rescaled to standardized ranges
707 used here.
708 ¶ Probability that parameter is different from zero between 0.05 and 0.10. Probability of unmarked parameters < 0.05.
709 § Probability that parameter is different from zero > 0.

710
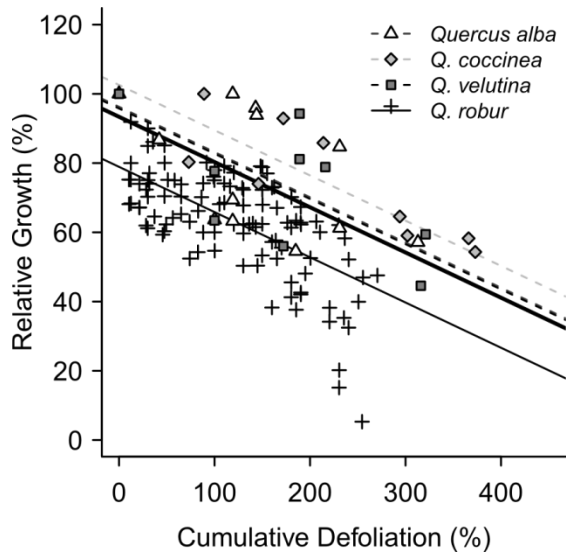
711
712
713

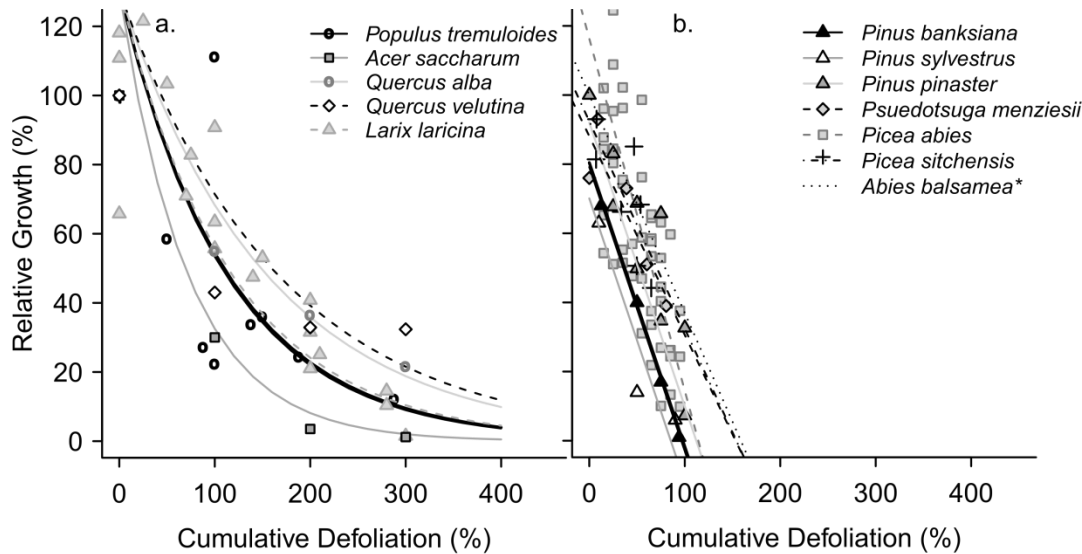714 **Figure 1.** Growth response of *Quercus* species to *Lymantria dispar* (L.) (gypsy moth) defoliation

715 including *Quercus robur* (Rubstov 1996), *Q. velutina* (Baker 1941), *Q. rubra* (Wargo 1981), and

716 *Quercus alba* (Baker 1941, Wargo 1981). Lines show best fit mixed model (Appendix S3, Table

717 S3-1). The best combined *Quercus* model varied intercepts but not slopes.

718

719

Figure 2. Growth decreases curvilinearly in response to defoliation (a.) in *Populus tremuloides*

(Rose 1958), manually defoliated juvenile trees of *Acer saccharum*, *Q. alba*, and *Q. velutina*

(Wargo 1981)*,* and *Larix laricina* (Ives and Nairn 1966). Growth of conifer species declined

linearly (b.) and included steep declines in *Pinus banksiana*, *P. pinaster*, *P. sylvestrus* with

slower declines in *Pseudotsuga menziesii, Picea abies,* and *Abies balsamea*. The best fit mixed

model in (a., lines) randomly varied slopes but not intercepts (Appendix S3, Table S3-1). Lines

in (b.) show model fits from Table 1 and the best mixed model for *Pinus* species that varied

intercept, but not slope (Appendix). *A. balsamea* relationship was published by Dobesberger

1998.

729
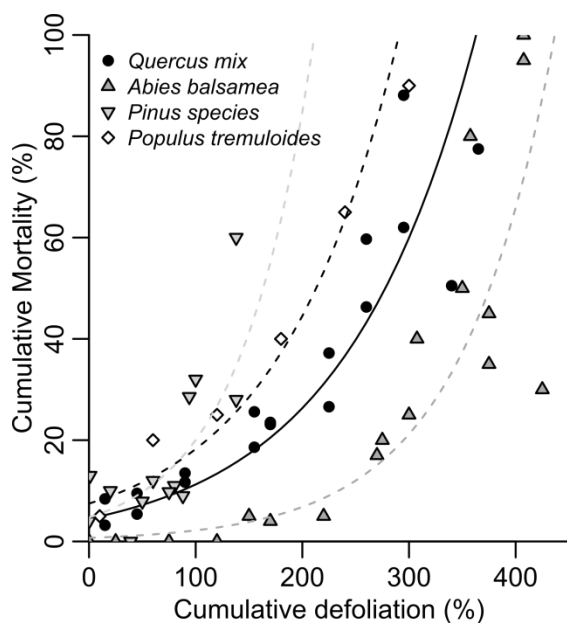
Figure 3. Cumulative mortality increased exponentially in response to accumulated defoliation.

Mortality rates rise most quickly in *Pinus* (Baker 1941, Kulman et al. 1963, Gross 1992),

followed by diffuse-porous *Populus* (Mann et al. 2007), and then ring-porous *Quercus*

dominated forests (Feicht et al. 1993). Mortality in *Abies* appears to rise more slowly (Blais

1958, Batzer 1973), but defoliation in this system is defined differently as damage by foliage

age-class. Lines show model fits from Table 2. All plots can be found in Appendix S2.

736